SANDIA REPORT

SAND2004-3535
Unlimited Release
Printed December 2004

Photovoltaic Array Performance Model

D.L. King, W.E. Boyson, J.A. Kratochvill

Prepared by
Sandia National Laboratories
Albuquerque, New Mexico 87185 and Livermore, California 94550

Sandia is a multiprogram laboratory operated by Sandia Corporation,
a Lockheed Martin Company, for the United States Department of Energy's
National Nuclear Security Administration under Contract DE-AC04-94AL85000.

Issued by Sandia National Laboratories, operated for the United States Department of Energy by Sandia Corporation.

Available to DOE and DOE contractors from
U.S. Department of Energy
Office of Scientific and Technical Information
P.O. Box 62
Oak Ridge, TN 37831

Telephone: (865)576-8401
Facsimile: (865)576-5728
E-Mail: reports@adonis.osti.gov
Online ordering: http://www.osti.gov/bridge

Available to the public from
U.S. Department of Commerce
National Technical Information Service
5285 Port Royal Rd
Springfield, VA 22161

Telephone: (800)553-6847
Facsimile: (703)605-6900
E-Mail: orders@ntis.fedworld.gov
Online order: http://www.ntis.gov/help/ordermethods.asp?loc=7-4-0#online

SAND2004-3535
Unlimited Release
Printed August 2004

Photovoltaic Array Performance Model

David L. King, William E. Boyson, Jay A. Kratochvil
Photovoltaic System R&D Department
Sandia National Laboratories
P. O. Box 5800
Albuquerque, New Mexico 87185-0752

Abstract

This document summarizes the equations and applications associated with the photovoltaic array performance model developed at Sandia National Laboratories over the last twelve years. Electrical, thermal, and optical characteristics for photovoltaic modules are included in the model, and the model is designed to use hourly solar resource and meteorological data. The versatility and accuracy of the model has been validated for flat-plate modules (all technologies) and for concentrator modules, as well as for large arrays of modules. Applications include system design and sizing, 'translation' of field performance measurements to standard reporting conditions, system performance optimization, and real-time comparison of measured versus expected system performance.

ACKNOWLEDGEMENTS

The long evolution of our array performance model has greatly benefited from valuable interactions with talented people from a large number of organizations. The authors would like to acknowledge several colleagues from the following organizations: AstroPower (Jim Rand, Michael Johnston, Howard Wenger, John Cummings), ASU/PTL (Bob Hammond, Mani Tamizhmani), BP Solar (John Wohlgemuth, Steve Ransom), Endecon (Chuck Whitaker, Tim Townsend, Jeff Newmiller, Bill Brooks), EPV (Alan Delahoy), Entech (Mark O'Neil), First Solar (Geoff Rich), FSEC (Gobind Atmaram, Leighton Demetrius), Kyocera Solar (Steve Allen), Maui Solar (Michael Pelosi), NIST (Hunter Fanney), NREL (Ben Kroposki, Bill Marion, Keith Emery, Carl Osterwald, Steve Rummel), Origin Energy (Pierre Verlinden, Andy Blakers), Pacific Solar (Paul Basore), PBS Specialties (Pete Eckert), PowerLight (Dan Shugar, Adrianne Kimber, Lori Mitchell), PVI (Bill Bottenberg), RWE Schott Solar (Miles Russell, Ron Gonsiorawski), Shell Solar (Terry Jester, Alex Mikonowicz, Paul Norum), SolarOne (Moneer Azzam), SunSet Technologies (Jerry Anderson), SWTDI (Andy Rosenthal, John Wiles), and Sandia (Michael Quintana, John Stevens, Barry Hansen, James Gee).

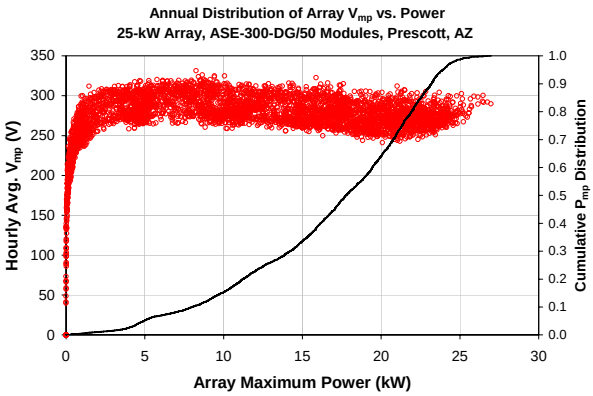

CONTENTS

This page intentionally left blank

INTRODUCTION

This document provides a detailed description of the photovoltaic module and array performance model developed at Sandia National Laboratories over the last twelve years. The performance model can be used in several distinctly different ways. It can be used to design (size) a photovoltaic array for a given application based on expected power and/or energy production on an hourly, monthly, or annual basis [1]. It can be used to determine an array power 'rating' by 'translating' measured parameters to performance at a standard reference condition. It can also be used to monitor the actual versus predicted array performance over the life of the photovoltaic system, and in doing so help diagnose problems with array performance.

The performance model is empirically based; however, it achieves its versatility and accuracy from the fact that individual equations used in the model are derived from individual solar cell characteristics. The versatility and accuracy of the model has been demonstrated for flat-plate modules (all technologies) and for concentrator modules, as well as for large arrays of modules. Electrical, thermal, solar spectral, and optical effects for photovoltaic modules are all included in the model [2, 3]. The performance modeling approach has been well validated during the last seven years through extensive outdoor module testing, and through inter-comparison studies with other laboratories and testing organizations [4, 5, 6, 7, 8]. Recently, the performance model has also demonstrated its value during the experimental performance optimization of off-grid photovoltaic systems [9, 10].

In an attempt to make the performance model widely applicable for the photovoltaic industry, Sandia conducts detailed outdoor performance tests on commercially available modules, and a database of the associated module performance parameters is maintained on the Sandia website (http://www.sandia.gov/pv). These module parameters can be used directly in the performance model described in this report. The module database is now widely used by a variety of module manufacturers and system integrators during system design and field testing activities. The combination of performance model and module database has also been incorporated in commercially available system design software [11]. In addition, it is now being considered for incorporation in other building and system energy modeling programs, including DOE-2 [12], Energy-10 [13], and the DOE-sponsored PV system analysis model (PV SunVisor) that is now being developed at NREL.

PERFORMANCE EQUATIONS FOR PHOTOVOLTAIC MODULES

The objective of any testing and modeling effort is typically to quantify and then to replicate the measured phenomenon of interest. Testing and modeling photovoltaic module performance in the outdoor environment is complicated by the influences of a variety of interactive factors related to the environment and solar cell physics. In order to effectively design, implement, and monitor the performance of photovoltaic systems, a performance model must be able to separate and quantify the influence of all significant factors. This testing and modeling challenge has been a goal of our research effort for several years.

The wasp-shaped scatter plot in Figure 1 illustrates the complexity of the modeling challenge using data recorded for a recent vintage 165-W_p multi-crystalline silicon module over a five day period in January 2002 during both clear sky and cloudy/overcast conditions. The vertical spread in the P_{mp} values is primarily caused by changes in the solar irradiance level, with lesser influences from solar spectrum, module temperature, and solar cell electrical properties. The horizontal spread in the associated V_{mp} values is primarily caused by module temperature, with lesser influences from solar irradiance and solar cell electrical properties. Our performance model effectively separates these influences so that the chaotic behavior shown in Figure 1 can be modeled with well-behaved relationships, as will be demonstrated in subsequent charts.

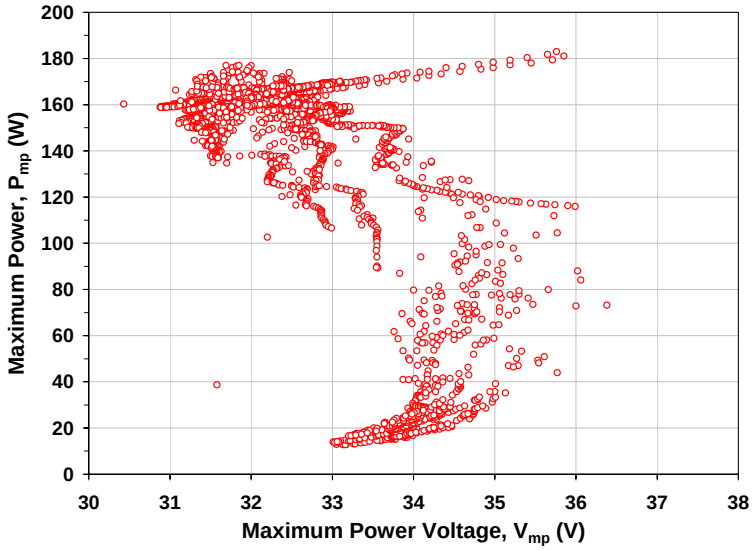

Figure 1. Scatter plot of over 3300 performance measurements recorded on five different days in January in Albuquerque with both clear sky and cloudy/overcast operating conditions for a 165-W_p mc-Si module.

Basic Equations

The following equations define the model used by the Solar Technologies Department at Sandia for analyzing and modeling the performance of photovoltaic modules. The equations describe the electrical performance for individual photovoltaic modules, and can be scaled for any series or parallel combination of modules in an array. The same equations apply equally well for individual cells, for individual modules, for large arrays of modules, and for both flat-plate and concentrator modules.

The form of the model given by Equations (1) through (10) is used when calculating the expected power and energy produced by a module, assuming that predetermined module performance coefficients and solar resource information are available. The solar resource and weather data required by the model can be obtained from tabulated databases or from direct measurements. The three classic points on a module current-voltage (I-V) curve, short-circuit current, open-circuit voltage, and the maximum-power point, are given by the first four equations. Figure 2 illustrates these three points, along with two additional points that better define the shape of the curve.

$$I_{sc} = I_{sco} \cdot f_1(AM_a) \cdot \{(E_b \cdot f_2(AOI) + f_d \cdot E_{diff}) / E_o\} \cdot \{1 + \alpha_{Isc} \cdot (T_c - T_o)\} \quad (1)$$

$$I_{mp} = I_{mpo} \cdot \{C_0 \cdot E_e + C_1 \cdot E_e^2\} \cdot \{1 + \alpha_{Imp} \cdot (T_c - T_o)\} \quad (2)$$

$$V_{oc} = V_{oco} + N_s \cdot \delta(T_c) \cdot \ln(E_e) + \beta_{Voc}(E_e) \cdot (T_c - T_o) \quad (3)$$

$$V_{mp} = V_{mpo} + C_2 \cdot N_s \cdot \delta(T_c) \cdot \ln(E_e) + C_3 \cdot N_s \cdot \{\delta(T_c) \cdot \ln(E_e)\}^2 + \beta_{Vmp}(E_e) \cdot (T_c - T_o) \quad (4)$$

$$P_{mp} = I_{mp} \cdot V_{mp} \quad (5)$$

$$FF = P_{mp} / (I_{sc} \cdot V_{oc}) \quad (6)$$

where:

$$E_e = I_{sc} / [I_{sco} \cdot \{1 + \alpha_{Isc} \cdot (T_c - T_o)\}] \quad (7)$$

$$\delta(T_c) = n \cdot k \cdot (T_c + 273.15) / q \quad (8)$$

The two additional points on the I-V curve are defined by Equations (9) and (10). The fourth point (I_x) is defined at a voltage equal to one-half of the open-circuit voltage, and the fifth (I_{xx}) at a voltage midway between V_{mp} and V_{oc}. The five points provided by the performance model provide the basic shape of the I-V curve and can be used to regenerate a close approximation to the entire I-V curve in cases where an operating voltage other than the maximum-power-voltage is required. For example, in battery charging applications, the system's operating voltage may be forced by the battery's state-of-charge to a value other than V_{mp}.

$$I_x = I_{xo} \cdot \{C_4 \cdot E_e + C_5 \cdot E_e^2\} \cdot \{1 + (\alpha_{Isc}) \cdot (T_c - T_o)\} \quad (9)$$

$$I_{xx} = I_{xxo} \cdot \{C_6 \cdot E_e + C_7 \cdot E_e^2\} \cdot \{1 + (\alpha_{Imp}) \cdot (T_c - T_o)\} \quad (10)$$

The following six sections of this document discuss all parameters and coefficients used in the equations above that define the performance model. These sections include discussions and definitions of parameters associated with basic electrical characteristics, irradiance dependence, solar resource, standard reporting conditions, temperature dependence, and module operating temperature.

Module Parameter Definitions

I_{sc} = Short-circuit current (A)
I_{mp} = Current at the maximum-power point (A)
I_x = Current at module V = $0.5 \cdot V_{oc}$, defines 4th point on I-V curve for modeling curve shape
I_{xx} = Current at module V = $0.5 \cdot (V_{oc} + V_{mp})$, defines 5th point on I-V curve for modeling curve shape
V_{oc} = Open-circuit voltage (V)
V_{mp} = Voltage at maximum-power point (V)
P_{mp} = Power at maximum-power point (W)

FF = Fill Factor (dimensionless)
N_s = Number of cells in series in a module's cell-string
N_p = Number of cell-strings in parallel in module
k = Boltzmann's constant, 1.38066E-23 (J/K)
q = Elementary charge, 1.60218E-19 (coulomb)
T_c = Cell temperature inside module (°C)
T_o = Reference cell temperature, typically 25°C
E_o = Reference solar irradiance, typically 1000 W/m^2
$\delta(T_c)$ = 'Thermal voltage' per cell at temperature T_c. For diode factor of unity (n=1) and a cell temperature of 25ºC, the thermal voltage is about 26 mV per cell.

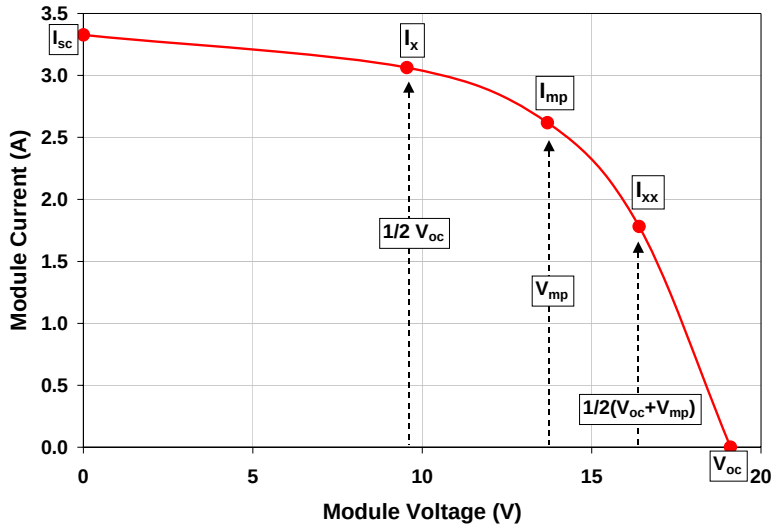

Figure 2. Illustration of a module I-V curve showing the five points on the curve that are provided by the Sandia performance model.

Irradiance Dependent Parameters

The following module performance parameters relate the module's voltage and current, and as a result the shape of the I-V curve (fill factor), to the solar irradiance level.

Figure 3 illustrates how the measured values for module V_{mp} and V_{oc} may vary as a function of the effective irradiance. In this example, the measured values previously shown in Figure 1 were first translated to a common temperature (50ºC) in order to remove temperature dependence. Then the coefficients (n, C_2, C_3) were obtained using regression analyses based on Equations (3) and (4). The coefficients were in turn used in our performance model to calculate voltage versus irradiance behavior at different operating temperatures. The validity of this modeling approach can be appreciated when it is recognized that the 3300 measured data points illustrated were recorded during both clear and cloudy conditions on five different days with solar irradiance from 80 to 1200 W/m^2 and module temperature from 6 to 45 ºC.

Figure 4 illustrates how the measured values for module current (I_{sc}, I_{mp}, I_x, I_{xx}) may vary as a function of the effective irradiance. Similar to the voltage analysis, the measured current values were translated to a common temperature to remove temperature dependence. The performance coefficients (C_0, C_1, C_4, C_5, C_6, C_7) associated with I_{mp}, I_x, and I_{xx} were then determined using regression analyses based on Equations (2), (9), and (10). Our formulation of the performance model uses the complexity associated with Equation (1) to account for any 'non-linear' behavior associated with I_{sc}. As a result, the plot of I_{sc} versus the 'effective irradiance' variable is always linear. The relationships for the other three current values can be nonlinear (parabolic) in order to closely match the I-V curve shape over a wide irradiance range. The formulation also takes advantage of the 'known' condition at an effective irradiance of zero, i.e. the currents are zero, thus helping make the model robust even at low irradiance conditions. The definitions for coefficients are as follows:

E_e = The 'effective' solar irradiance as previously defined by Equation (7). This value describes the fraction of the total solar irradiance incident on the module to which the cells inside actually respond. When tabulated solar resource data are used in predicting module performance, Equation (7) is used directly. When direct measurements of solar resource variables are used, then alternative procedures can be used for determining the effective irradiance, as discussed later in this document.
C_0, C_1 = Empirically determined coefficients relating I_{mp} to effective irradiance, E_e. $C_0+C_1 = 1$, (dimensionless)
C_2, C_3 = Empirically determined coefficients relating V_{mp} to effective irradiance (C_2 is dimensionless, and C_3 has units of 1/V)
C_4, C_5 = Empirically determined coefficients relating the current (I_x), to effective irradiance, E_e. $C_4+C_5 = 1$, (dimensionless)
C_6, C_7 = Empirically determined coefficients relating the current (I_{xx}) to effective irradiance, E_e. $C_6+C_7 = 1$, (dimensionless)
n = Empirically determined 'diode factor' associated with individual cells in the module, with a value typically near unity, (dimensionless). It is determined using measurements of V_{oc} translated to a common temperature and plotted versus the natural logarithm of effective irradiance. This relationship is typically linear over a wide range of irradiance (~0.1 to 1.4 suns).

Parameters Related to Solar Resource

For system design or sizing purposes, the solar irradiance variables required by the performance model are typically obtained from a database or meteorological model providing estimates of hourly-average values for solar resource and weather data [14, 15]. These solar irradiance data can be manipulated using different methods in order to calculate the expected solar irradiance incident on the surface of a photovoltaic module positioned in an orientation that depends on the system design and application [16, 17]. On the other hand, for field testing or for long-term performance monitoring, the solar irradiance in the plane of the module is often a measured value and should be used directly in the performance model.

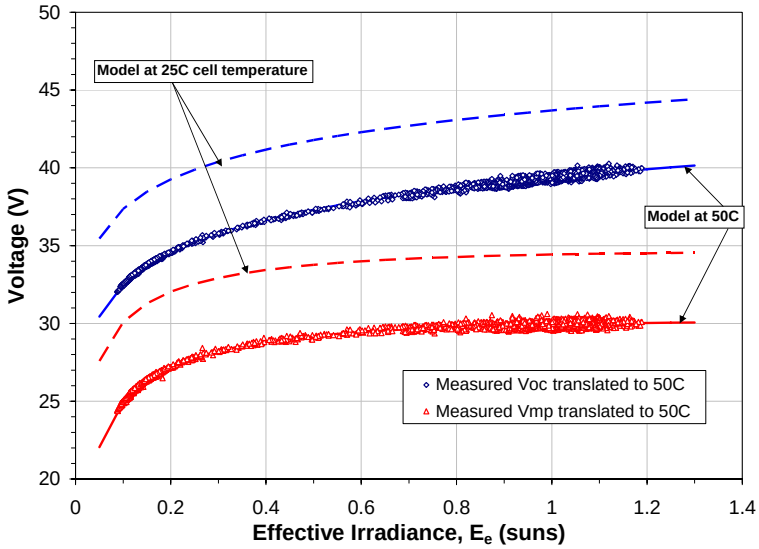

Figure 3. Over 3300 measurements recorded on five different days with both clear sky and cloudy/overcast operating conditions for 165-W_p mc-Si module. Measured values for V_{oc} and V_{mp} were translated to a common temperature, 50°C. Regression analyses provided coefficients used in the performance model used to predicted curves at different operating conditions.

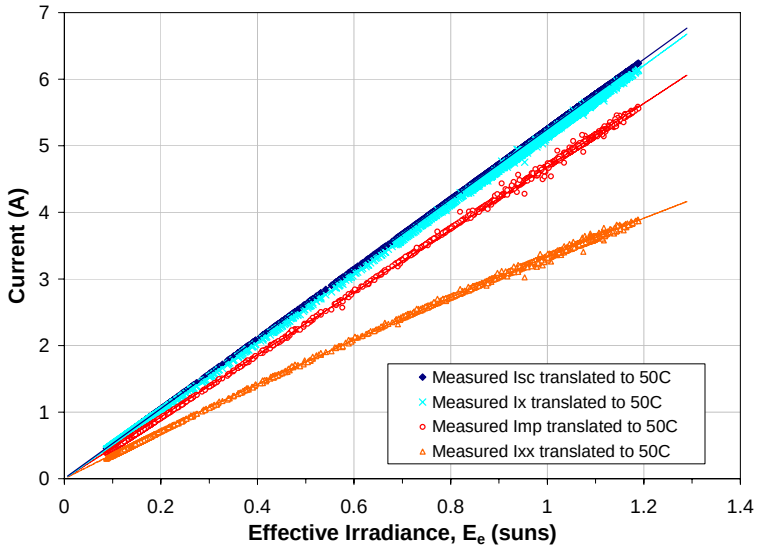

Figure 4. Over 3300 measurements recorded on five different days with both clear sky and cloudy/overcast operating conditions for 165-W_p mc-Si module. Measured values for currents were translated to a common temperature, 50°C, prior to regression analysis.

The empirical functions $f_1(AM_a)$ and $f_2(AOI)$ quantify the influence on module short-circuit current of variation in the solar spectrum and the optical losses due to solar angle-of-incidence. These functions are determined by a module testing laboratory using explicit outdoor test procedures [2, 8]. The intent of these two functions is to account for systematic effects that

occur on a recurrent basis during the predominantly clear conditions when the majority of solar energy is collected. For example, Figure 5 illustrates how the solar spectral distribution varies as the day progresses from morning toward noon, resulting in a systematic influence on the normalized short-circuit current of a typical Si cell. For crystalline silicon modules, the normalized I_{sc} is typically several percent higher at high air mass conditions than it is at solar noon. The effects of intermittent clouds, smoke, dust, and other meteorological occurrences can for all practical purposes be considered random influences that average out on a weekly, monthly, or annual basis. For modules from the same manufacturer, these two empirical functions can often be considered 'generic', as long as the cell type and module superstrate material (e.g., glass) are the same. Figures 6 and 7 illustrate typical examples for the empirically determined functions.

It can be seen in Figure 6 that the influence of the changing solar spectrum is relatively small for air mass values between 1 and 2. In the context of annual energy production, it should also be recognized that over 90% of the solar energy available over an entire year occurs at air mass values less than 3. So, the spectral influence illustrated at air mass values higher than 3 is of somewhat academic importance for the system designer. As documented elsewhere [1], the cumulative effect of the solar spectral influence on annual energy production is typically quite small, less than 3%. Nonetheless, using our modeling approach, it is straightforward to include the systematic influence of solar spectral variation.

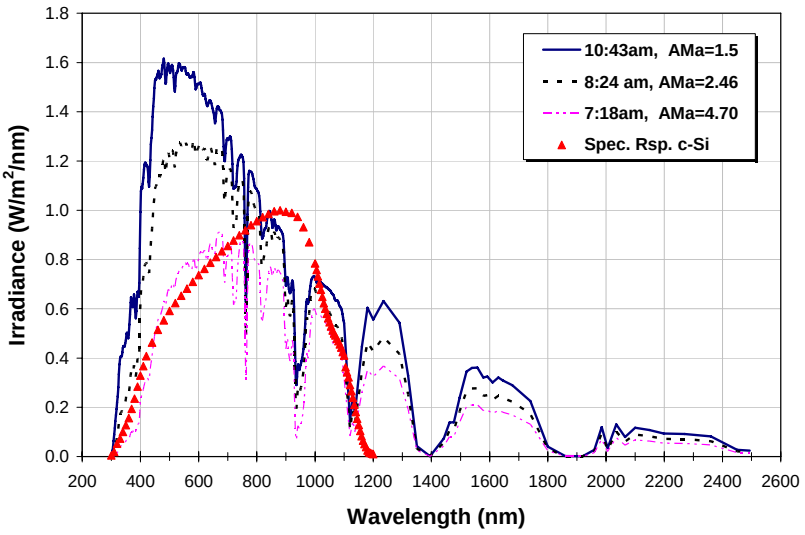

Figure 5. Measured solar spectral irradiance on a clear day in Davis, CA, at different air mass conditions during the day. The normalized spectral response of a typical silicon solar cell is superimposed for comparison.

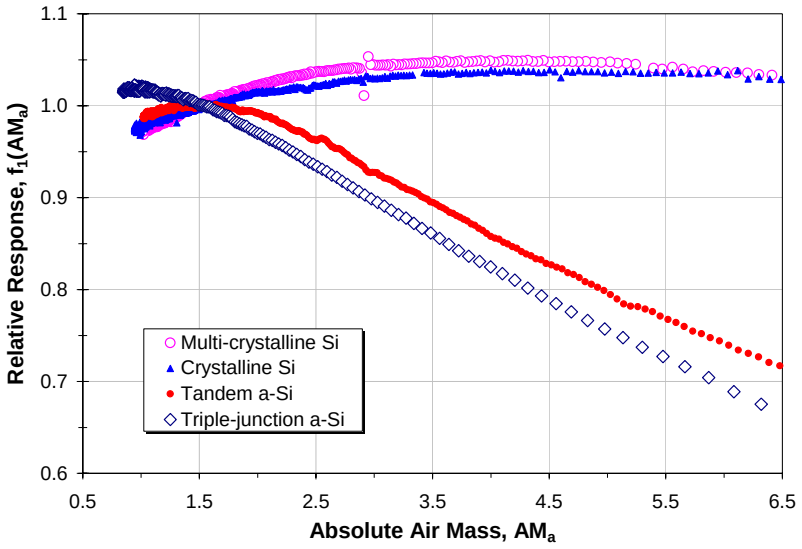

Figure 6. Typical empirical relationship illustrating the influence of solar spectral variation on module short-circuit current, relative to the AM_a=1.5 reference condition. Results were measured at Sandia National Laboratories for a variety of commercial modules.

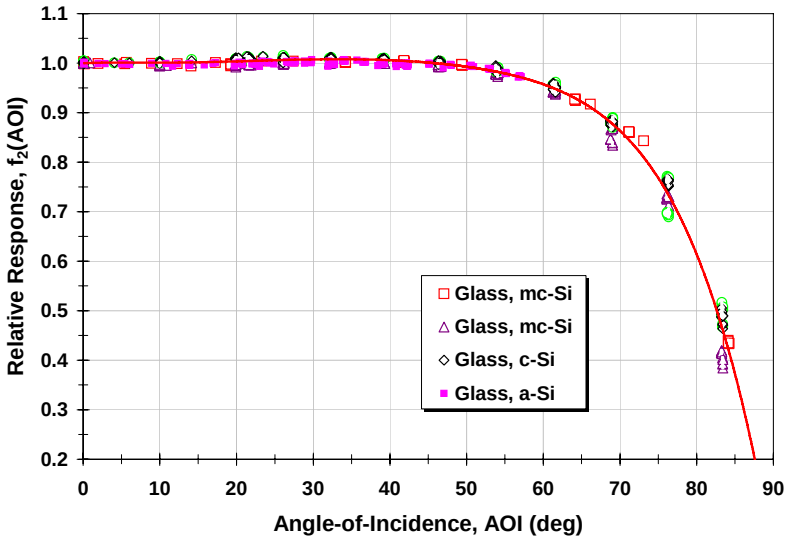

Figure 7. Typical empirical relationship illustrating the influence of solar angle-of-incidence in reducing a module's short-circuit-current. Results were measured at Sandia National Laboratories for four different module manufacturers. The effect is dominated by the reflectance characteristics of the glass surface.

Figure 7 shows that the influence of optical (reflectance) losses for flat-plate modules is typically negligible until the solar angle-of-incidence is greater than about 55 degrees. This loss is in addition to the typical 'cosine' loss for a module surface that is not oriented perpendicular to the path of sunlight. The cumulative effect (loss) over the year should be considered for different system designs and module orientations. For modules that accurately track the sun, there is no optical loss. In the case of a vertically oriented flat-plate module in the south wall of a building, the annual energy loss due to optical loss is about 5% [1].

Our performance model is also directly applicable to concentrator photovoltaic modules. In this case, the empirical functions, $f_1(AM_a)$ and $f_2(AOI)$, take on somewhat greater roles. The effects of solar spectral influence, variation in optical efficiency over the day, module misalignment, and non-linear behavior of I_{sc} versus irradiance can all be adequately accounted for in $f_1(AM_a)$. As previously discussed, the intent of these empirically-determined relationships is to account for the bulk of the effect of known systematic influences, with the assumption that other uncontrollable factors result in random effects that average out over the year. For concentrator modules, the term angle-of-incidence can be considered synonymous with 'tracking error.' Therefore, using predetermined coefficients, the $f_2(AOI)$ function can be used to quantify the effect of tracking error on concentrator module performance. The definitions for parameters are as follows:

$E_b = E_{dni} \cos(AOI)$, beam component of solar irradiance incident on the module surface, (W/m^2)
E_{diff} = Diffuse component of solar irradiance incident on the module surface, (W/m^2)
f_d = Fraction of diffuse irradiance used by module, typically assumed to be 1 for flat-plate modules. For point-focus concentrator modules, a value of zero is typically assumed, and for low-concentration modules a value between zero and 1 can be determined.
E_e = "Effective" irradiance to which the PV cells in the module respond, (dimensionless, or "suns")
E_o = Reference solar irradiance, typically 1000 W/m^2, with ASTM standard spectrum.
AM_a = Absolute air mass, (dimensionless). This value is calculated from sun elevation angle and site altitude, and it provides a relative measure of the path length the sun must travel through the atmosphere, AM_a=1 at sea level when the sun is directly overhead.
AOI = Solar angle-of-incidence, (degrees). AOI is the angle between a line perpendicular (normal) to the module surface and the beam component of sunlight.
T_c = Temperature of cells inside module, (°C). Typically determined from module back surface temperature measurements, or from a thermal model using solar resource and environmental data.
$f_1(AM_a)$ = Empirically determined polynomial relating the solar spectral influence on I_{sc} to air mass variation over the day, where:

$$f_1(AM_a) = a_0 + a_1 \cdot AM_a + a_2 \cdot (AM_a)^2 + a_3 \cdot (AM_a)^3 + a_4 \cdot (AM_a)^4$$

$f_2(AOI)$ = Empirically determined polynomial relating optical influences on I_{sc} to solar angle-of-incidence (AOI), where:

$$f_2(AOI) = b_0 + b_1 \cdot AOI + b_2 \cdot (AOI)^2 + b_3 \cdot (AOI)^3 + b_4 \cdot (AOI)^4 + b_5 \cdot (AOI)^5$$

Parameters at Standard Reporting (Reference) Conditions

Standard Reporting Conditions are used by the photovoltaic industry to 'rate' or 'specify' the performance of the module. This rating is provided at a single standardized (reference) operating condition [18, 19]. The associated performance parameters are typically either manufacturer's nameplate ratings (specifications) or test results obtained from a module testing laboratory. The accuracy of these performance specifications is critical to the design of photovoltaic arrays and systems because they provide the reference point from which performance at all other operating conditions is derived. The consequence of a 10% error in the module performance rating will be a 10% effect on the annual energy production from the photovoltaic system. System integrators and module manufacturers should make every effort to ensure the accuracy of module performance ratings. The performance parameters and conditions associated with the standard reporting condition are defined as follows:

T_o = Reference cell temperature for rating performance, typically 25°C
E_o = Reference solar irradiance, typically 1000 W/m^2
$I_{sco} = I_{sc}(E = E_o$ W/m^2, $AM_a = 1.5$, $T_c = T_o$ °C, AOI = 0°) (A)
$I_{mpo} = I_{mp}(E_e = 1, T_c = T_o)$ (A)
$V_{oco} = V_{oc}(E_e = 1, T_c = T_o)$ (V)
$V_{mpo} = V_{mp}(E_e = 1, T_c = T_o)$ (V)
$I_{xo} = I_x(E_e = 1, T_c = T_o)$ (A)
$I_{xxo} = I_{xx}(E_e = 1, T_c = T_o)$ (A)

Temperature Dependent Parameters

Although not universally recognized or standardized, the use of four separate temperature coefficients is instrumental in making our performance model versatile enough to apply equally well for all photovoltaic technologies over the full range of operating conditions. Currently standardized procedures erroneously assume that the temperature coefficient for V_{oc} is applicable for V_{mp} and the temperature coefficient for I_{sc} is applicable for I_{mp} [18]. If not available from the module manufacturer, the required parameters are available from the module database or can be measured during outdoor tests in actual operating conditions [3]. In addition, our performance model allows the temperature coefficients for voltage (V_{oc} and V_{mp}) to vary with solar irradiance, if necessary. For example, a concentrator silicon cell may have a V_{oc} temperature coefficient of –2.0 mV/°C at 1X concentration, but at 200X concentration the value may drop to –1.7 mV/°C. However, for non-concentrator flat-plate modules, constant values for the voltage temperature coefficients are generally adequate.

The definitions for parameters are as follows, and when used in the performance model defined in this document, the engineering units for the temperature coefficients must be as specified below in order to be consistent with the equations.

α_{Isc} = Normalized temperature coefficient for I_{sc}, (1/°C). This parameter is 'normalized' by dividing the temperature dependence (A/°C) measured for a particular standard solar spectrum and irradiance level by the module short-circuit current at the standard reference

condition, I_{sco}. Using these (1/°C) units makes the same value applicable for both individual modules and for parallel strings of modules.

α_{Imp} = Normalized temperature coefficient for I_{mp}, (1/°C). Normalized in the same manner as α_{Isc}.

$\beta_{Voc}(E_e) = \beta_{Voco} + m_{\beta Voc} \cdot (1-E_e)$, (V/°C) Temperature coefficient for module open-circuit-voltage as a function of the effective irradiance, E_e. Usually, the irradiance dependence can be neglected and β_{Voc} is assumed to be a constant value.

β_{Voco} = Temperature coefficient for module V_{oc} at a 1000 W/m^2 irradiance level, (V/°C)

$m_{\beta Voc}$ = Coefficient providing the irradiance dependence for the V_{oc} temperature coefficient, typically assumed to be zero, (V/°C).

$\beta_{Vmp}(E_e) = \beta_{Vmpo} + m_{\beta Vmp} \cdot (1-E_e)$, (V/°C) Temperature coefficient for module maximum-power-voltage as a function of effective irradiance, E_e. Usually, the irradiance dependence can be neglected and β_{Vmp} is assumed to be a constant value.

β_{Vmpo} = Temperature coefficient for module V_{mp} at a 1000 W/m^2 irradiance level, (V/°C)

$m_{\beta Vmp}$ = Coefficient providing the irradiance dependence for the V_{mp} temperature coefficient, typically assumed to be zero, (V/°C).

Module Operating Temperature (Thermal Model)

When designing a photovoltaic system it is necessary to predict its expected annual energy production. To do so, a thermal model is required to estimate module operating temperature based on the local environmental conditions; solar irradiance, ambient temperature, wind speed, and perhaps wind direction. Site-dependent solar resource and meteorological data from recognized databases [14] or from meteorological models [15] are typically used to provide the environmental information required in the array design analysis. Estimates of hourly-average values for solar irradiance, ambient temperature, and wind speed are used in the thermal model to predict the associated operating temperature of the photovoltaic module. There is uncertainty associated with both the tabulated environmental data and the thermal model, but this approach has proven adequate for system design purposes.

After a system has been installed, the solar irradiance and module temperature can be measured directly and the results used in the performance model. The measured values avoid the inherent uncertainty associated with estimating module temperature based on environmental parameters, and improve the accuracy of the performance model for continuously predicting expected system performance.

In the mid-1980s, a thermal model was developed at Sandia for system engineering and performance modeling purposes [20]. Although rigorous, this early model has proven to be unnecessarily complex, not applicable to all module technologies, and not easily adaptable to site dependent influences.

A simpler empirically-based thermal model, described by Equation (11), was more recently developed at Sandia. The model has been applied successfully for flat-plate modules mounted in an open rack, for flat-plate modules with insulated back surfaces simulating building integrated situations, and for concentrator modules with finned heat sinks. The simple model has proven to

be very adaptable and entirely adequate for system engineering and design purposes by providing the expected module operating temperature with an accuracy of about ±5°C. Temperature uncertainties of this magnitude result in less than a 3% effect on the power output from the module.

The empirically determined coefficients (a, b) used in the model are determined using thousands of temperature measurements recorded over several different days with the module operating in a near thermal-equilibrium condition (nominally clear sky conditions without temperature transients due to intermittent cloud cover). The coefficients determined are influenced by the module construction, the mounting configuration, and the location and height where wind speed is measured.

The standard meteorological practice for recording wind speed and direction locates the measurement device (anemometer) at a height of 10 meters in an area with a minimum number of buildings or structures obstructing air movement. The tabulated wind speed and direction data provided in meteorological databases were recorded under these conditions. However, it should be noted that by analyzing data recorded after system installation, the thermal model can be 'fine tuned' by determining new coefficients (a,b) that compensate for site dependent influences and anemometer installations different from standard meteorological practice.

$$T_m = E \cdot \left\{ e^{a+b \cdot WS} \right\} + T_a \tag{11}$$

where:

T_m = Back-surface module temperature, (°C).
T_a = Ambient air temperature, (°C)
E = Solar irradiance incident on module surface, (W/m^2)
WS = Wind speed measured at standard 10-m height, (m/s)
a = Empirically-determined coefficient establishing the upper limit for module temperature at low wind speeds and high solar irradiance
b = Empirically-determined coefficient establishing the rate at which module temperature drops as wind speed increases

Figure 8 illustrates typical measured data recorded on six different days with nominally clear conditions and a wide range of irradiance, wind speed, and wind direction. The module in this case was a large-area 300-W model with tempered-glass front and back surfaces. The effect of non-equilibrium 'heat up' periods (~ 30-min duration) is illustrated for two mornings when the sun first illuminated the module. A linear fit to the measured data provided the intercept and slope (a, b) coefficients required in the model. After the coefficients have been determined for a specific module then it is also possible to calculate the nominal operating cell temperature (NOCT) specified by ASTM [18], as well as the module temperature associated with the commonly used PVUSA Test Condition (PTC) [19].

Wind direction can also have a small but noticeable influence on module operating temperature. However, incorporating the effect of wind direction in the thermal model is believed to be unnecessarily complex. Therefore, in our approach the influence of wind direction on operating temperature is regarded as a random influence adding some uncertainty to the thermal model, but also tending to average out on an annual basis. Similarly, thermal transients caused by clouds and the module's heat capacitance can introduce random influences on module temperature, but again these random effects average out on a daily or annual basis.

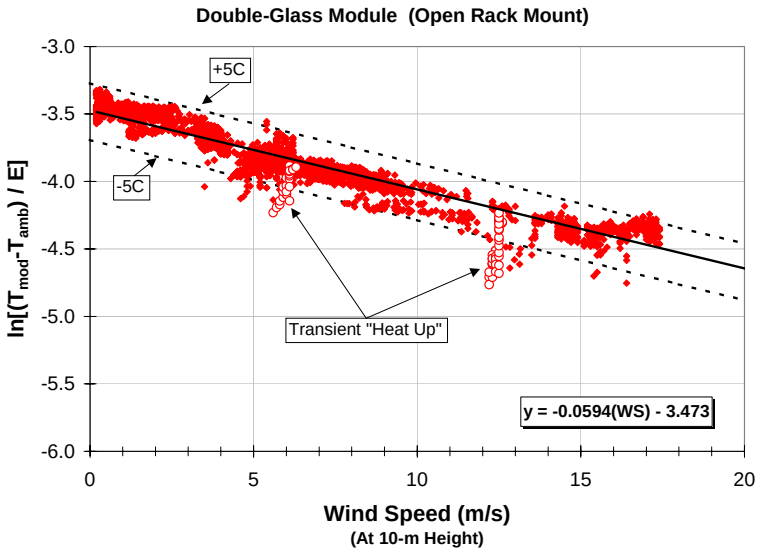

Figure 8. Experimentally determined relationship for back surface temperature of a flat-plate module in an open-rack mounting configuration as a function of solar irradiance, ambient temperature and wind speed. A linear regression fit to the data provides the coefficients (a, b) for the thermal model.

Cell temperature and back-surface module temperature can be distinctly different, particularly for concentrator modules. The temperature of cells inside the module can be related to the module back surface temperature through a simple relationship. The relationship given in Equation (12) is based on an assumption of one-dimensional thermal heat conduction through the module materials behind the cell (encapsulant and polymer layers for flat-plate modules, ceramic dielectric and aluminum heat sink for concentrator modules). The cell temperature inside the module is then calculated using a measured back-surface temperature and a predetermined temperature difference between the back surface and the cell.

$$T_c = T_m + \frac{E}{E_o} \cdot \Delta T \tag{12}$$

where:

T_c = Cell temperature inside module, (°C)
T_m = Measured back-surface module temperature, (°C).
E = Measured solar irradiance on module, (W/m^2)
E_o = Reference solar irradiance on module, (1000 W/m^2)

ΔT = Temperature difference between the cell and the module back surface at an irradiance level of 1000 W/m^2. This temperature difference is typically 2 to 3 °C for flat-plate modules in an open-rack mount. For flat-plate modules with a thermally insulated back surface, this temperature difference can be assumed to be zero. For concentrator modules, this temperature difference is typically determined between the cell and the root of a finned heat exchanger (heat sink) on the back of the module.

Table 1 provides empirically-determined coefficients found to be representative of different module types and mounting configurations. The cases in the table can be considered generic for typical flat-plate photovoltaic modules from different manufacturers. However, the thermal behavior of concentrator modules can vary significantly, depending on the module design. Therefore, coefficients for concentrators must be empirically determined for each module design. One example, for a 1994-vintage linear-focus concentrator module, is given in the table.

Table 1. Empirically determined coefficients used to predict module back surface temperature as a function of irradiance, ambient temperature, and wind speed. Wind speed was measured at the standard meteorological height of 10 meters.

Module Type	Mount	a	b	ΔT (°C)
Glass/cell/glass	Open rack	-3.47	-.0594	3
Glass/cell/glass	Close roof mount	-2.98	-.0471	1
Glass/cell/polymer sheet	Open rack	-3.56	-.0750	3
Glass/cell/polymer sheet	Insulated back	-2.81	-.0455	0
Polymer/thin-film/steel	Open rack	-3.58	-.113	3
22X Linear Concentrator	Tracker	-3.23	-.130	13

PERFORMANCE EQUATIONS FOR ARRAYS

Equations (1) through (10) can also be used for arrays composed of many modules by simply accounting for the series and parallel combinations of modules in the array. If the number of modules connected in series in a module-string is M_s, then multiply the voltages calculated using Equations (3) and (4) by M_s. If the number of module-strings connected in parallel in the array is M_p, then multiply the currents calculated using Equations (1), (2), (9), and(10) by M_p. The calculated array performance using this approach is based on the expected performance of the individual modules, and as a result may be slightly optimistic because other array-level losses such as module mismatch and wiring resistance are not included.

Ideally, performance (I-V) measurements at the array level are available, in which case the accuracy of the performance model can be further improved. Array measurements can provide the four basic performance parameters (I_{sco}, I_{mpo}, V_{oco}, V_{mpo}) at the standard reporting (reference) condition, as well as the eight other coefficients (C_0, C_1, …, C_7). The spectral influence, f1(AM_a), the optical losses, f2(AOI), and the temperature coefficients for the array are assumed to be available from test results on individual modules. Using array measurements, the electrical performance of the entire array can be modeled completely, in which case the model directly includes the array-level losses associated with module mismatch and wiring resistance that are difficult to predict or determine explicitly. In essence, the array is modeled as if it were a very large module. Generally, the effect of mismatch and resistance losses is small (<5%) relative to performance expected from individual module nameplate ratings. Sandia's module database includes several arrays of modules that were characterized in this manner.

To illustrate the procedure used to determine array performance coefficients, as well as their subsequent use in modeling the expected energy production, results for a 3.4-kW_p system located in Albuquerque, New Mexico, will be presented.

Array Performance Example

The 3.4-kW_p array evaluated was composed of two parallel module-strings, each with 24 crystalline silicon modules (70 W_p) connected in series. There were 864 silicon cells in series in each module-string. The array was connected to a 2.5-kW inverter, and the system was connected to the local utility grid. Field performance measurements (I-V curves) were recorded on one clear morning in July using a portable curve tracer and two different solar irradiance sensors (pyranometers).

The first, most important, and perhaps most difficult challenge during array performance characterization is to determine an accurate value for the array short-circuit current (I_{sco}) at a desired reference condition. After I_{sco} has been determined, the remainder of the array performance analysis becomes self consistent and straight forward. The most commonly used reference condition is defined by the ASTM [18]. Nominally, the ASTM condition represents a clear sky condition with the sun at a mid-elevation angle in the sky and a module temperature of 25°C. The actual array operating condition during testing is determined by four factors: solar irradiance composed of a beam and a diffuse component, solar spectrum, solar angle-of-incidence, and array temperature. The typical effects of solar spectrum and angle-of-incidence on module performance were previously illustrated in Figures 6 and 7. The influence of these factors on the response of different pyranometers is documented elsewhere [23].

Figure 9 illustrates measured values for array I_{sc} translated to a common temperature and plotted as a function of plane-of-array solar irradiance, as measured by two different pyranometers. The Kipp & Zonen pyranometer had a thermopile sensor and the LICOR pyranometer had a silicon photodiode sensor. The response of these pyranometers was influenced by the same factors affecting the array short-circuit current; but the magnitude of the effect for each factor differed between pyranometers and both pyranometers differed from the array. Therefore, even though the data illustrated were recorded during a calm perfectly clear day, the results indicate

systematic trends rather than nice linear behavior versus measured irradiance. The most practical way to approach these field measurements is to first recognize there are a variety of interacting factors present in the measured data and then select the time period during the day when the combined effect of the factors is minimized, as illustrated in Figure 9.

Figure 10 shows the measured current values (I_{sc}, I_{mp}, I_x, I_{xx}) translated to a common temperature and plotted as a function of the effective irradiance, E_e. The effective irradiance for each measurement was calculated using the measured I_{sco} value and Equation (7). Alternative methods for determining the effective irradiance during field testing are discussed later in this report. The measured data illustrated are typically well behaved, and regression analyses are used to obtain the associated modeling coefficients.

Figures 11 and 12 show the measured array voltages (V_{oc}, V_{mp}) translated to a common temperature versus the effective irradiance. Regression analyses using these measured data provided the coefficients required to model the voltage behavior of the array, in a manner exactly analogous to that used for individual modules. Note that the independent variables used are different in these two cases which facilitates the determination of the modeling coefficients. The performance coefficients obtained are given in the charts.

Figure 13 illustrates the effectiveness of the performance model after the determination of the required coefficients. This chart illustrates the modeled V_{oc} and V_{mp} as a function of effective irradiance for two different operating temperatures, 25°C and 50°C. The measured values for V_{oc} and V_{mp}, after translation to 50°C, are also shown on the chart for comparison with the model.

As a final illustration of the effectiveness of the performance model, Figure 14 shows the most relevant array performance parameter, namely maximum power, as a function of effective irradiance and cell temperature. The performance model was used to calculate P_{mp} for three different cell temperatures. In addition, the field measurements were shown along with the modeled results. The chart also illustrates the single operating condition corresponding to the ASTM Standard Reporting Condition. Other performance models have not achieved the accuracy demonstrated by this example, particularly when the wide range for solar irradiance is considered.

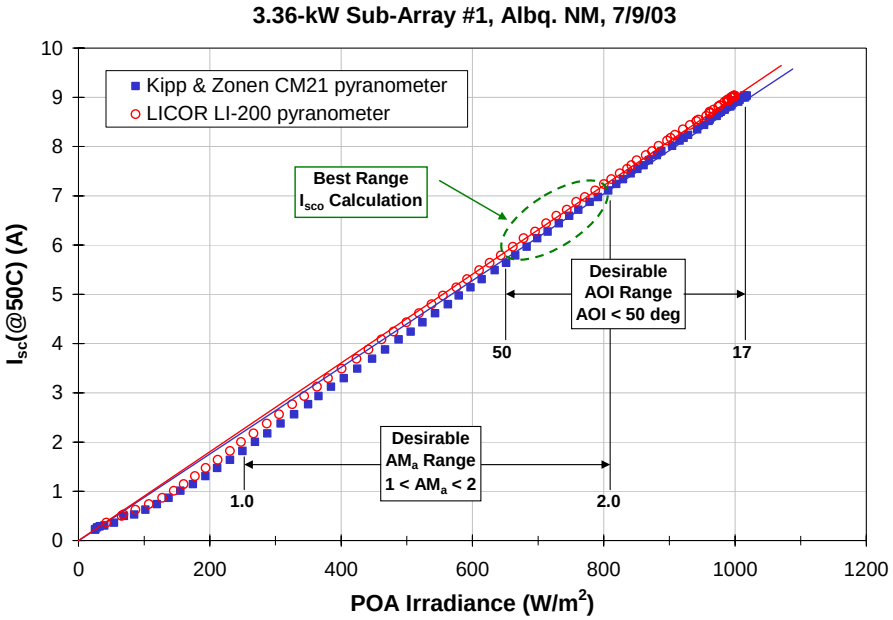

Figure 9. Method used to obtain an accurate field measurement of the reference short-circuit current, I_{sco}, for the array. Data recorded during the time of day when the combined effect of solar spectrum and angle-of-incidence is smallest should be used for determining I_{sco}.

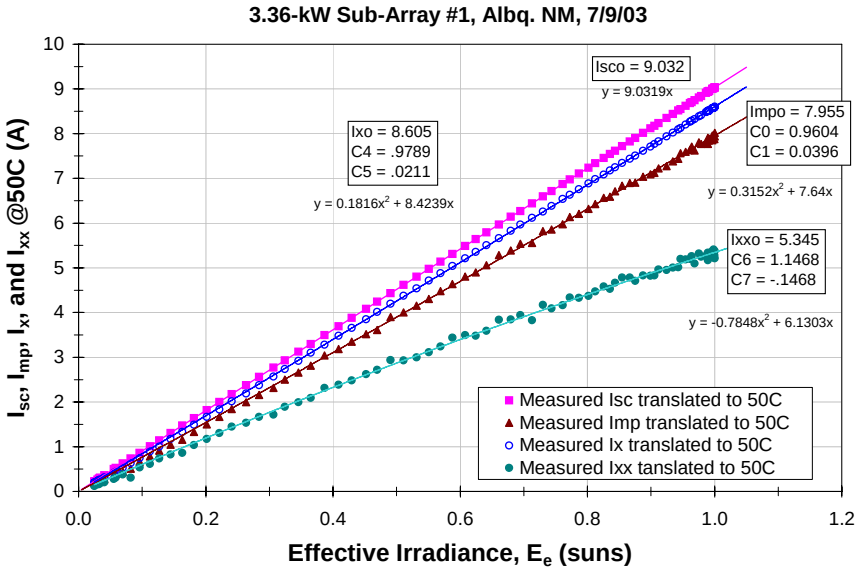

Figure 10. Array current measurements recorded on a clear day for a 3.4-kWp array of c-Si modules in Albuquerque, New Mexico. The measured values were translated to a common temperature, 50°C, before the regression analyses used to determine performance coefficients.

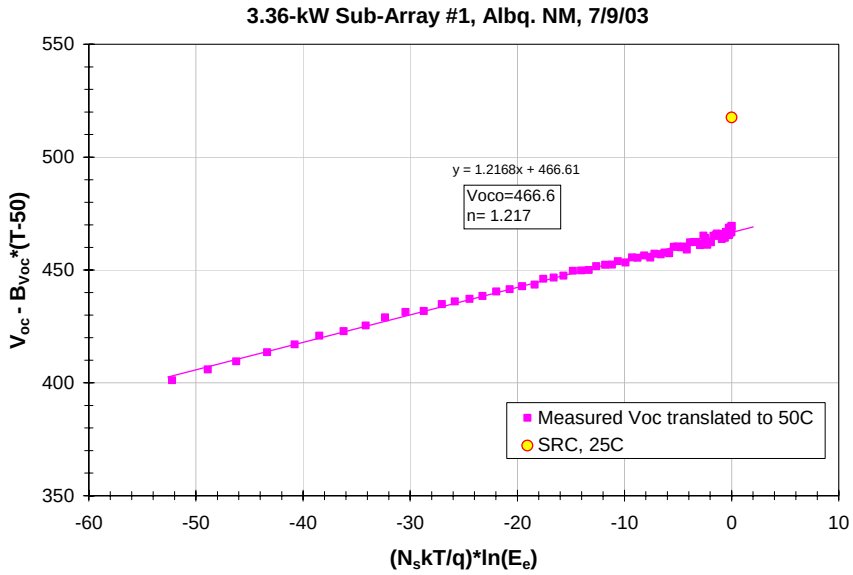

Figure 11. Regression analysis used to determine performance coefficients for array open-circuit voltage. The measured V_{oc} values were translated to a common temperature, 50°C, before the regression analysis. The reference V_{oc} value at the ASTM Standard Reporting Condition is also shown. N_s = 864 for this array.

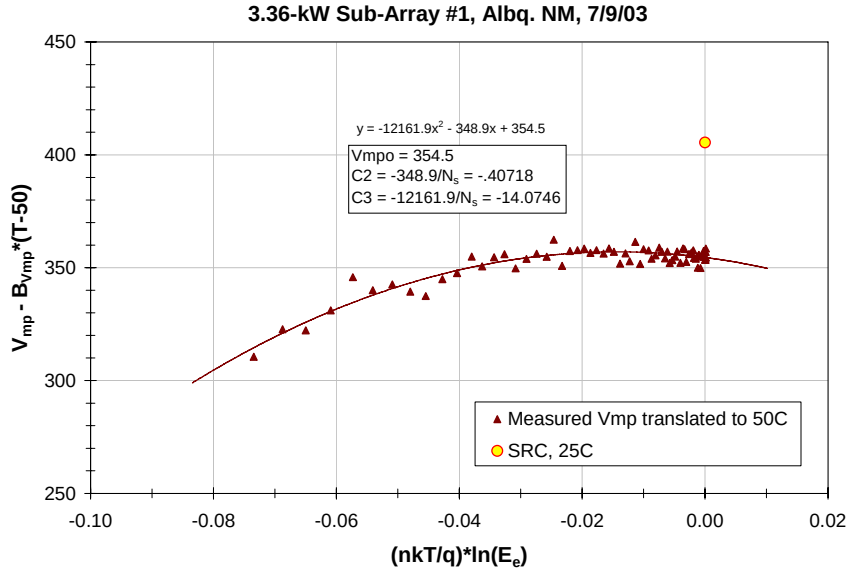

Figure 12. Regression analysis used to determine performance coefficients for array maximum-power voltage. The measured V_{mp} values were translated to a common temperature, 50°C, prior to the regression analysis. The reference V_{mp} value at the ASTM Standard Reporting Condition is also shown. Trend line coefficients must be divided by N_s to obtain C_2, C_3 coefficients.

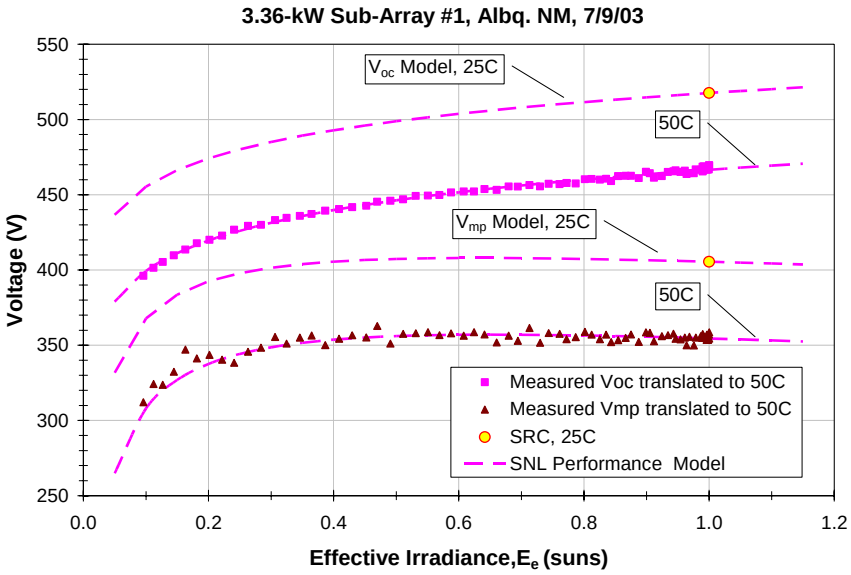

Figure 13. Array voltages given by performance model after determination of required modeling coefficients. For comparison, the measured values were translated to a common temperature, 50°C, and also included on the chart. The modeled performance values at the ASTM Standard Reporting Condition are also shown.

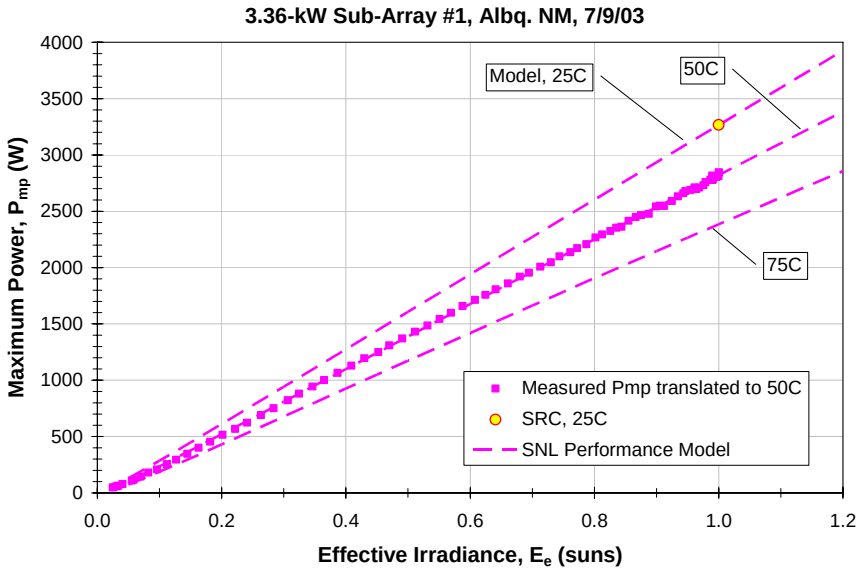

Figure 14. Modeled maximum power from array at three operating temperatures as a function of effective irradiance. Field measurements translated to 50ºC are shown for comparison with model. The reference P_{mp} value at the ASTM Standard Reporting Condition is also shown.

Grid-Connected System Energy Production

After the determination of the array performance coefficients, the expected energy production for the array and for the system can be accurately modeled on an hourly, daily, monthly, or annual basis. To do so, the array performance model must be coupled with a database of typical-meteorological-year (TMY) solar resource and weather data, or with direct measurements of the required parameters.

For the grid-connected system previously discussed, the chart in Figure 15 illustrates the calculated dc-energy available from the array on a monthly basis. In this case, hourly-average values for solar irradiance and for module temperature were used in the array performance model. The chart also shows the calculated ac-energy available from the system where the performance characteristics (efficiency versus power level) for the inverter were included in the analysis. This particular system was also instrumented with a data acquisition system to measure ac-energy production; so the measured ac-energy production over the same period is also shown for comparison with the model.

The information presented in Figure 15 illustrates several system performance characteristics that were highlighted by the array performance model. First, the energy loss associated with inverter efficiency is evident as the difference between the predicted array dc-energy and the measured ac-energy. For the first several months of operation (June through October 2002), the inverter was overheating which unnecessarily reduced its efficiency. The inverter self limits input power when the power available from the array exceeds the inverter's rating and when the inverter's circuitry exceeds a maximum allowable temperature. A cooling fan for the inverter was installed in October 2002. Then, an unrelated module wiring failure occurred in December 2002 that removed one of the two module-strings from the circuit, effectively cutting the measured ac-energy in half; the wiring problem was repaired in January 2003. The following four months of operation (February through May 2003) show good inverter efficiency and excellent agreement between predicted and measured ac-energy production.

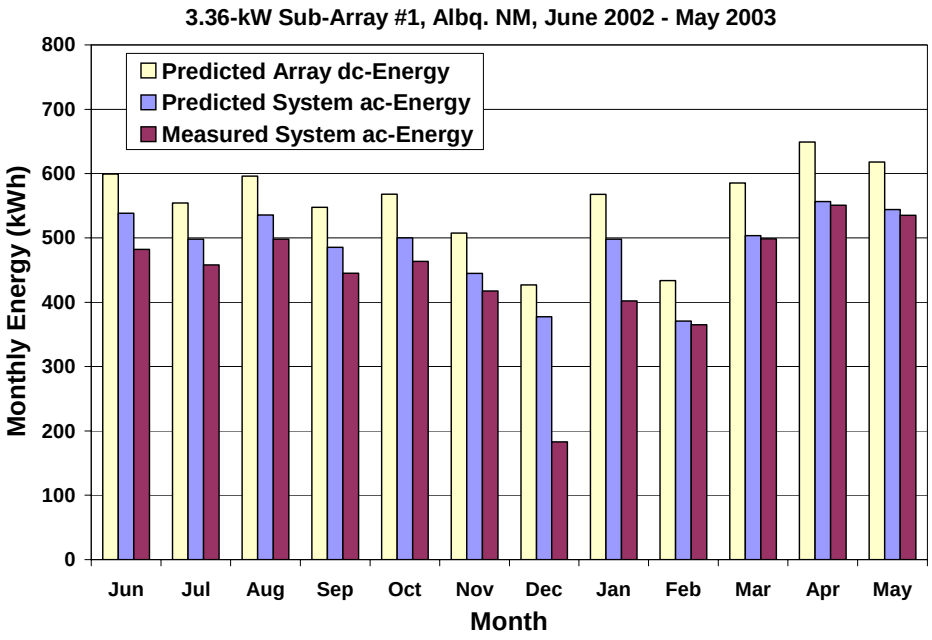

Figure 15. Comparison of predicted and measured monthly energy production for a 3.36-kW grid-connected photovoltaic system in Albuquerque, NM. Chart shows predicted dc-energy available from the array, as well as the predicted and measured ac-energy provided by the system.

Figure 16 is more complex but provides additional information for the system integrator that is useful when sizing the array and when selecting compatible system components. The chart provides a scatter plot of calculated hourly values for the two performance parameters, P_{mp} and V_{mp}, of most interest to the system designer. The scatter illustrates the expected range for these values for an entire year. The cumulative dc-energy curve gives the fraction of the total annual energy as a function of the maximum-power level of the array. For instance, approximately 55% of the annual dc-energy available from the array occurs at maximum-power levels below 2.5 kW. Superimposed on the scatter chart are the operating requirements for the system's inverter. The inverter's maximum-power-point-tracking (MPPT) capability functions in the range from 250 V_{dc} to 550 V_{dc}, which nicely matches the array's annual range for V_{mp}. On the other hand, the inverter's upper limit for dc input power was 2.7 kW; therefore, the chart shows many hours during the year when the power available from the array exceeded the inverter's input limit. This situation does not damage the inverter, the inverter limits its input power, but it does result in power available from the array not being utilized. Analyses of this type can be used both in the design phase for systems and later when monitoring their performance after installation.

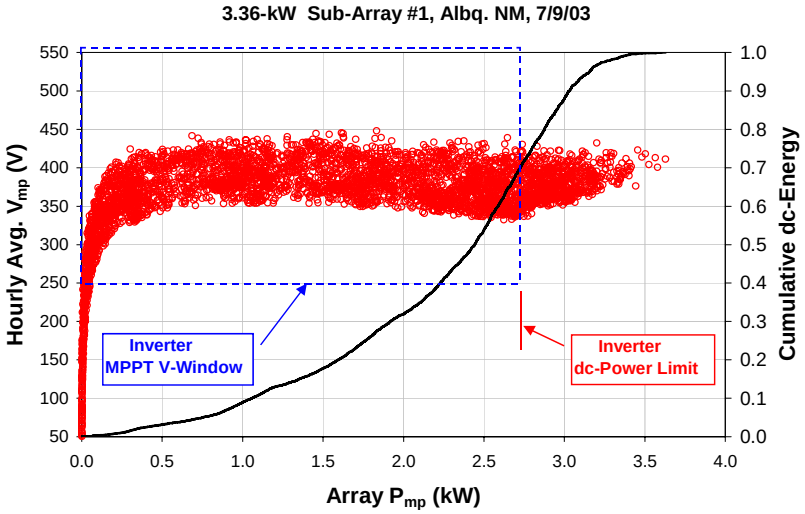

Figure 16. Scatter chart of calculated hourly-average performance values for 3.36-kW array in Albuquerque, NM, over a one-year period. The 'window' superimposed shows the voltage and power constraints for the inverter used with the system. The fraction of the cumulative annual energy available from the array is also shown as a function of the array power level.

Off-Grid System Optimization

The array performance model can also be used during the design and subsequent performance optimization for off-grid photovoltaic systems. These systems are more complex than grid-connected systems because they include energy storage (batteries) and frequently auxiliary power sources (generators). As a result of this complexity an accurate array performance model is highly beneficial in fully understanding their performance. A comprehensive example illustrating off-grid system optimization has been documented elsewhere [9, 10].

'TRANSLATING' ARRAY MEASUREMENTS TO STANDARD CONDITIONS

It is often desired to verify or 'rate' array or module performance (power) by recording an I-V measurement in the field at an arbitrary operating condition, and then 'translating' the measurement to the ASTM Standard Reporting Condition [18] or to the PVUSA PTC condition [19]. Historically the ASTM standard procedure used to perform these translations has been problematic. It has provided less than desirable accuracy because all the factors influencing the shape of I-V curve were not accounted for. The accuracy of the ASTM translation procedure varies significantly depending on the photovoltaic technology considered. Recent work by NREL has improved upon the historic ASTM procedure when a family of I-V curves at different irradiance and temperature levels are available for a module of interest [21]. The Sandia performance model coupled with parameters from the module database provides a well-established alternative that has been demonstrated to work well for all commercially available module and array technologies.

Translation Equations

The performance equations previously given have been rewritten below as Equations (13) through (20). This form of the performance model can be used to 'translate' measurements at an arbitrary test condition to performance at a desired reporting (reference) condition. In addition, these equations are applicable to a single cell, a single module, a module-string with multiple modules connected in series, and to an array with multiple module-strings connected in parallel. The equations use coefficients from the module database that are matched to the modules in the array being evaluated. The performance model was designed to make it unnecessary to account for the number of modules or module-strings connected in parallel. However, for the voltage translation equations to work correctly, it is necessary to specify how many modules are connected in series in each module-string.

$$I_{sco} = I_{sc} / [E_e \cdot \{1+\alpha_{Isc} \cdot (T_c - T_o)\}] \quad (13)$$

$$I_{mpo} = I_{mp} / [\{1 + \alpha_{Imp} \cdot (T_c - T_o)\} \cdot \{C_0 \cdot E_e + C_1 \cdot E_e^2\}] \quad (14)$$

$$V_{oco} = V_{oc} - M_s \cdot N_s \cdot \delta(T_c) \cdot \ln(E_e) - M_s \cdot \beta_{Voc}(E_e) \cdot (T_c - T_o) \quad (15)$$

$$V_{mpo} = V_{mp} - C_2 \cdot M_s \cdot N_s \cdot \delta(T_c) \cdot \ln(E_e) - C_3 \cdot M_s \cdot N_s \cdot \{\delta(T_c) \cdot \ln(E_e)\}^2 - M_s \cdot \beta_{Vmp}(E_e) \cdot (T_c - T_o) \quad (16)$$

$$P_{mpo} = I_{mpo} \cdot V_{mpo} \quad (17)$$

$$FF_o = P_{mpo} / (I_{sco} \cdot V_{oco}) \quad (18)$$

$$I_{xo} = I_x / [\{1 + (\alpha_{Isc}) \cdot (T_c - T_o)\} \cdot \{C_4 \cdot E_e + C_5 \cdot E_e^2\}] \quad (19)$$

$$I_{xxo} = I_{xx} / [\{1 + (\alpha_{Imp}) \cdot (T_c - T_o)\} \cdot \{C_6 \cdot E_e + C_7 \cdot E_e^2\}] \quad (20)$$

where:

M_s = Number of modules connected in series in each module-string

T_c = Cell temperature inside module, °C. This value can be refined using Eqn. (12) by starting with measurements of back-surface module temperature.

E_e = 'Effective' irradiance, which can be determined in different ways as discussed later in this document.

Other parameters are the same as previously defined for individual modules.

Analysis of Module-String V_{oc} Measurements

During the installation and diagnostic testing of large arrays, module-string open-circuit voltage (V_{oc}) measurements are probably the easiest and most common measurement used to obtain a quick assessment of electrical performance. With a little extra effort, these quick measurements can be more diagnostic and instructive than typically recognized. If recorded periodically over the life of a photovoltaic system, these measurements also provide a defensible metric for tracking array performance degradation rates. Figure 17 illustrates the practicality of module-string V_{oc} measurements where the wiring for seventeen module-strings is terminated in the same 'combiner box' making it possible to record module-string V_{oc} measurements for a large array within minutes using a portable meter. The value of this procedure will be illustrated with an example.

Figure 17. Photo of a wiring 'combiner box' housing the terminations for 17 high-voltage module-strings in a large array. In this case, each module string had twelve 150-W_p crystalline silicon modules connected in series.

It is possible to 'translate' an accurate (±1%) module-string V_{oc} measurement to the value at the Standard Reporting Condition with a resulting uncertainty less than ±2%. This translation is accomplished by simultaneously recording reasonably accurate (±10%) values for the effective solar irradiance and for module temperature (±3°C) and then applying Equation (15).

For commercial modules of the same type, the production variation in the module open-circuit voltage is typically relatively small (< ±2%), and the nameplate specification, V_{oco}, is also typically accurate (±2%). Therefore, after translation, the measured module-string V_{oc} values can be critically examined relative to expected values. Since there is no current flow in an open-circuit condition, the variability observed between translated module-string voltages does not contain the effects of module or wiring resistance or module-to-module mismatch in module power ratings. Rather, the values are a direct assessment of the health of all the solar cells in the module-string. If a translated module-string V_{oc} is more than 5% lower than expected based on the module nameplate value, then it is likely that one or more modules in the module-string are below specification. In addition, the variation from the average module-string V_{oc} should not be more than about ±3%.

Figure 18 illustrates the distribution of measured values, after translation, for 12 module-strings in a large array of crystalline silicon modules. Each module-string had twelve 150-W_p crystalline silicon modules wired in series. The expected (nameplate) module-string V_{oc} is shown along with a ±5% tolerance band the system integrator might realistically expect to contain the results for all module-strings. Repeating this measurement procedure on an annual basis provides a convenient method for early detection of module or wiring problems, and the results can be used to establish degradation trends over the life of the system.

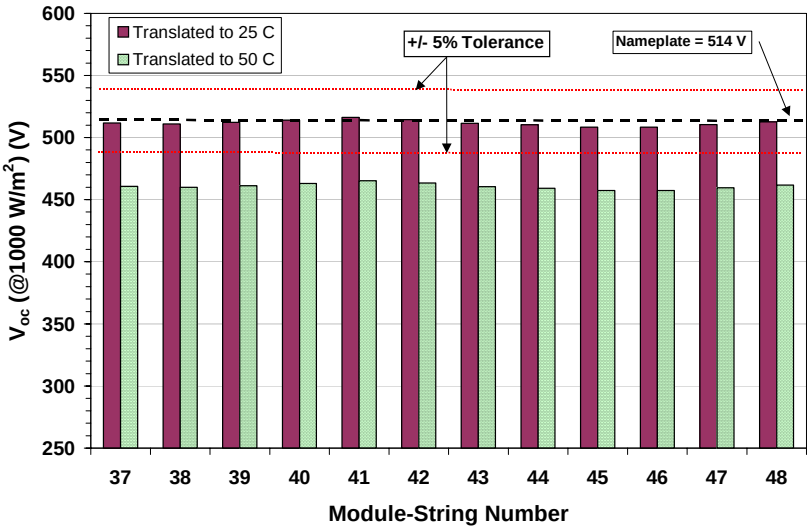

Figure 18. Example of module-string V_{oc} measurements translated to the Standard Reporting Condition for comparison to expected nameplate value. Module-strings had twelve 150-W_p c-Si modules in series. The translation to a 50ºC temperature is also shown for comparison.

Analysis of Array Operating Current and Voltage

Photovoltaic system integrators and owners need a convenient method for comparing the power actually provided by an array with the expected power level. This comparison is needed immediately after installation to validate initial system performance, as well as over the long-term as the system ages. Direct measurement of the array I-V characteristics on a periodic basis is often not practical because of the cost associated with the testing effort. For very large arrays, it may not be possible to directly measure the I-V characteristics of the entire array because of the limitations of the test equipment. Therefore, a convenient low-cost alternative is needed for monitoring array performance. Such an alternative can be implemented by using the array performance model in conjunction with measurements of array operating current and voltage.

In order to implement this performance monitoring procedure, four measured values must be available: array operating current (I_{op}), operating voltage (V_{op}), effective irradiance (E_e), and module temperature (T_c). In some cases, the operating current and voltage may be available directly from the power conditioning equipment (inverter). Otherwise, all four measured values can be obtained from a dedicated data acquisition system. If in addition the power conditioning electronics effectively track the maximum-power-point of the array over the day, then I_{op} and V_{op} can be considered equivalent to I_{mp} and V_{mp}.

Given the four measured values, the array performance model can be used in two ways to verify the array is generating the expected power. First, the measured values can be translated using Equations (14), (16), and (17) to the expected values at the Standard Reporting Condition. The calculated values for I_{mpo}, V_{mpo}, and P_{mpo} then provide a continuous relative comparison with

either the array nameplate specifications or with the initial values (ratings) obtained when the system was first installed. Second, the measured values for E_e and T_c can be used in Equations (2), (4), and (5) to calculate the expected values for I_{op} and V_{op} at that operating condition. These calculated values can then be compared in real time to the measured I_{op} and V_{op}.

By continuously or periodically analyzing these measured and calculated data, trends can be recorded that provide early warning of system performance anomalies, as well as long-term degradation rates. For instance, a day-to-day downward trend in the calculated I_{mpo} value could be caused by array soiling. A downward trend in the calculated V_{mpo} value over a period of weeks or years could be caused by a slow increase in the series resistance of module and/or cell interconnect wiring. The calculated and measured power values can also be integrated over a day, week, month, or year in order to provide a performance metric (index) based on system energy production.

DETERMINATION OF EFFECTIVE IRRADIANCE (E_e) DURING TESTING

When testing the performance of photovoltaic arrays, the largest source of error in power ratings is often associated with the instrument and procedure used to quantify the solar irradiance. The difficulty arises from several sources that produce systematic influences on test results: photovoltaic modules respond to only a portion of the solar spectrum as previously illustrated in Figure 5, devices used to measure solar irradiance may respond to all solar wavelengths or to a range similar to the photovoltaic modules, the optical acceptance angle or view angle of the module may differ significantly from that of the solar irradiance sensor, the response of both the module and the solar irradiance sensor vary significantly as a function of the solar angle-of-incidence, and the solar irradiance sensor and module may be mounted in a different orientations. The concept of 'effective solar irradiance' provides a method for addressing these systematic influences and reduces the difficulty and uncertainty associated with field testing photovoltaic arrays.

The initial objective during field performance testing and I-V curve translation should be to determine an accurate value for the 'effective irradiance' parameter, E_e. The 'effective irradiance' is the solar irradiance in the plane of the module to which the cells in the module actually respond, after the influences of solar spectral variation, optical losses due to solar angle-of-incidence, and module soiling are considered. Depending on the measured data available and the accuracy required, the effective irradiance can be determined using four different approaches, as discussed below.

After the E_e value has been determined using one of these four approaches, the performance parameters from the measured I-V curve can be translated to obtain the basic performance parameters at the Standard Reporting (Reference) Condition using Equations (13) through (20). In turn, the translated parameters can be used in Equations (1) through (10) to calculate expected array performance at all other operating conditions.

Detailed Laboratory Approach

The laboratory based approach for determining E_e during outdoor performance testing requires the determination of all factors in Equation (21). For individual modules in a testing laboratory, specific test procedures can be applied to quantify all parameters and coefficients required. In the lab, the separate components of the solar irradiance (beam and diffuse) are measured, and other tests are used to quantify three other related influences; solar spectral variation ($f_1(AM_a)$), solar angle-of-incidence ($f_2(AOI)$), and the relative response of the module to diffuse versus beam irradiance (f_d). The results of this detailed laboratory testing provide the coefficients tabulated in Sandia's module database. Fortunately, the coefficients determined for these three influences are also applicable for arrays of modules.

Therefore, when testing arrays using this approach, many of the predetermined module characteristics can be used, and it is then only necessary to measure the components of the solar irradiance, E_b and E_{diff}, where $E_b = E_{dni} \cdot \cos(AOI)$. In this case, the solar irradiance measurements are made using thermopile-based instruments (pyrheliometer and pyranometer) that respond to the full solar spectrum. The added complexity of separately measuring the direct normal irradiance and the diffuse irradiance, as well as calculating values for AOI and AM_a, make this approach relatively complicated to implement in the field. Therefore, the other three approaches discussed below will probably be more practical for most field testing purposes.

Equation (21) also includes a 'soiling factor' (SF) which accounts for the unavoidable soiling loss present when array performance measurements are made. SF has a value of 1.0 for a clean array, and is typically not less than 0.95 unless the array is visually quite dirty. The SF can be quantified in the field by measuring the I_{sc} of an individual module in the array before and after periodically cleaning it.

$$E_e = f_1(AM_a) \cdot \{(E_b \cdot f_2(AOI) + f_d \cdot E_{diff}) / E_o\} \cdot SF \qquad (21)$$

where:

$E_b = E_{dni} \cdot \cos(AOI)$

E_{dni} = Direct normal irradiance from pyrheliometer, (W/m^2)

Direct Measurement Using a Matching Reference Module

The most direct and arguably the most accurate way to determine E_e during array performance measurements is by using a calibrated 'reference' module. The reference module should be periodically recalibrated by a module testing laboratory. Ideally, this reference module should be of the same type used in the array being tested. At a minimum, the reference module should have the same cell type (matched spectral response) as the array, and should have the same construction in order to mimic the optical properties of the modules in the array. During testing, the reference module must be mounted in the same orientation as other modules in the array. With reasonable attention to detail during I-V curve measurements, and by accounting for array soiling, the repeatability of array performance determinations (ratings) at the Standard Reporting Conditions should be within ±3%.

Equation (22) is used to calculate E_e based on the measured short-circuit current for the reference module, I_{scr}, and the temperature of the reference module, T_{cr}. The calibration current for the reference module, I_{scor}, and its temperature coefficient, α_{Iscr} , are predetermined by a module testing laboratory. As in the previous approach, the soiling factor (SF) accounts for the array soiling loss during testing, assuming that the reference module is always kept clean. This reference module approach is particularly effective because it avoids measuring the separate components of solar irradiance, and it automatically accounts for solar spectral and solar angle-of-incidence influences, thus avoiding complexity and several possible sources for error.

Long-term array performance monitoring can be achieved by permanently mounting the reference module in the array. Assuming that measurements of I_{mp}, V_{mp}, and T_c are continuously available during system operation, then two approaches can be used for monitoring array power output over time. Measurements for E_e and for cell temperature, T_c, can be used to calculate the expected power output from the array using Equation (5), and then this value can be directly compared to the measured power indicated by the system's power conditioning equipment. Alternatively, the measured values for I_{mp} and V_{mp} can be translated to the Standard Reporting Condition using Equations (14) and (16) and used to establish a trend relative to the initial values determined when the system was first installed. If permanently mounted in the array, the reference module can also be used to quantify the soiling factor for the array by recording its I_{sc} measurements before and after cleaning it. If the reference module is permanently mounted in the array and not cleaned, then the SF factor should be removed from Equation (22) because the reference module is assumed to soil at the same rate as the rest of the array.

The reference module approach is also applicable for concentrator arrays. In this case, the reference module should be an individual cell packaged in a housing that replicates the construction and optics of the modules in the array. Ideally, the reference module should be mounted on a separate solar tracker with known tracking accuracy during concentrator array testing.

$$E_e = \{I_{scr} / [I_{scor} \cdot (1+\alpha_{Iscr} \cdot (T_{cr}-T_o))]\} \cdot SF \qquad (22)$$

Simplified Approach Using a Single Solar Irradiance Sensor

Solar irradiance sensors such as the thermopile-based pyranometers and pyrheliometers manufactured by Eppley Labs and Kipp & Zonen, as well as the photodiode-based pyranometer manufactured by LICOR, are widely used for quantifying the solar irradiance during array performance measurements. Historically, this approach for quantifying the solar irradiance has been the most commonly used, primarily because it is a logical progression from the laboratory-based comprehensive measurement approach previously discussed. Unfortunately, compromises associated with cost, calibration rigor, spectral and optical effects, and test procedures have often introduced errors in field testing that are larger than commonly recognized.

For instance, thermopile-based pyranometers are expensive, require careful calibration, and their calibration value can be strongly dependent on solar angle-of-incidence. These pyranometers accept light from a wider view-angle (larger AOI) than typical flat-plate modules, and unlike photovoltaic modules are insensitive to the spectral content of the sunlight. Typically, their angle-of-incidence behavior is ignored during field testing, and doing so can result in a 5 to 10% error in the solar irradiance measurement. Even larger measurement errors are likely if the solar angle-of-incidence is large (> 70 degrees). These measurement errors in irradiance are inadvertently but often translated into the same level of error in the calculated array performance rating. A single irradiance sensor is also incapable of distinguishing between the beam and the diffuse component of solar irradiance, which, as indicated in Equation (1), influence the array performance differently. (These sources for measurement error can be avoided by using the reference module approach, as previously discussed.)

Photodiode-based pyranometers have the advantage of being inexpensive, and as a result there are literally thousands in use for measuring solar irradiance associated with photovoltaic systems. However, they have the same shortcomings as the thermopile-based pyranometers, with the difference that, like photovoltaic modules, their response is influenced by the spectral content of the sunlight. The photodiode used in these pyranometers is typically a silicon device, and as a result has a spectral response that is similar to some silicon modules, but not all. The influence of solar angle-of-incidence on the response of these pyranometers does not match that of flat-plate modules; therefore, these pyranometers should not be considered an acceptable substitute for a 'matching reference module.' Procedures for improving the accuracy of these inexpensive devices have been documented elsewhere [22, 23], but even with these corrections, errors of 5 to 10% in array performance measurements are not uncommon.

Although we do not recommend this single pyranometer approach, we also recognize that it is the most common approach in use today. So, if the array owner is willing to accept the magnitude of measurement error introduced by ignoring the solar spectral and solar angle-of-incidence influences on the behavior of both the pyranometer and the photovoltaic array, then Equation (23) can be used to calculate the effective irradiance.

$$E_e = (E / E_o) \cdot SF \qquad (23)$$

where:

E = Solar irradiance indicated by irradiance sensor, (W/m^2)
E_o = Reference solar irradiance, typically 1000 W/m^2

Using a Predetermined Array Short-Circuit Current, I_{sco}

Assuming that an acceptably accurate value for the array short-circuit current, I_{sco}, at the Standard Reporting Condition has been previously determined, then it can be used in Equation (24) to calculate the effective irradiance. In this approach, the soiling factor is implicitly contained in the measured I_{sc} value and is not included separately in the equation. This simple approach provides a convenient method for using periodic array I-V measurements to assess array performance by applying Equations (13) through (20). One distinct advantage is that the need for a solar irradiance measurement is avoided, but a module temperature measurement is still required.

This approach provides a convenient method for monitoring array performance parameters over time, assuming that measured values for I_{sc}, I_{mp}, V_{oc}, V_{mp}, and T_c are available from I-V curve data, or directly from power conditioning hardware. Changes in the shape (FF) of the array I-V curve, as well as changes in the array V_{oc}, can be quantified without the need for solar irradiance measurements. For instance, if the array wiring becomes more resistive over time, the translated values for V_{mp} will have a downward trend. Similarly, if the fundamental characteristics of the solar cells degrade over time, then the translated values for V_{oc} will have a downward trend.

$$E_e = \{I_{sc} / [I_{sco} \cdot (1+\alpha_{Isc} \cdot (T_c - T_o))]\} \quad (24)$$

DETERMINATION OF CELL TEMPERATURE (T_C) DURING TESTING

The most direct method for determining cell temperature during field performance measurements is to attach multiple temperature sensors (thermocouples) to the back surface of modules in the array. Light gage thermocouples that do not perturb the temperature of the location being measured are preferable. Averaging the measurements provided by multiple temperature sensors can adequately compensate for spatial temperature variation present in the array. After an average back surface module temperature has been determined, then Equation (12) can be used to get an improved estimate of the average cell temperature inside the modules.

The influence of wind speed, wind direction, structural support members, module frames, and module junction boxes can introduce non-uniform temperature distributions across the array surface. Typically, these spatial temperature differences vary by less than 5 ºC. Figure 19 is an infrared (IR) thermal image of a small photovoltaic array illustrating a typical temperature distribution during sunny conditions with calm wind (< 3 m/s). Judicious placement of thermocouples will help in obtaining a more accurate value for the average module temperature during field performance measurements.

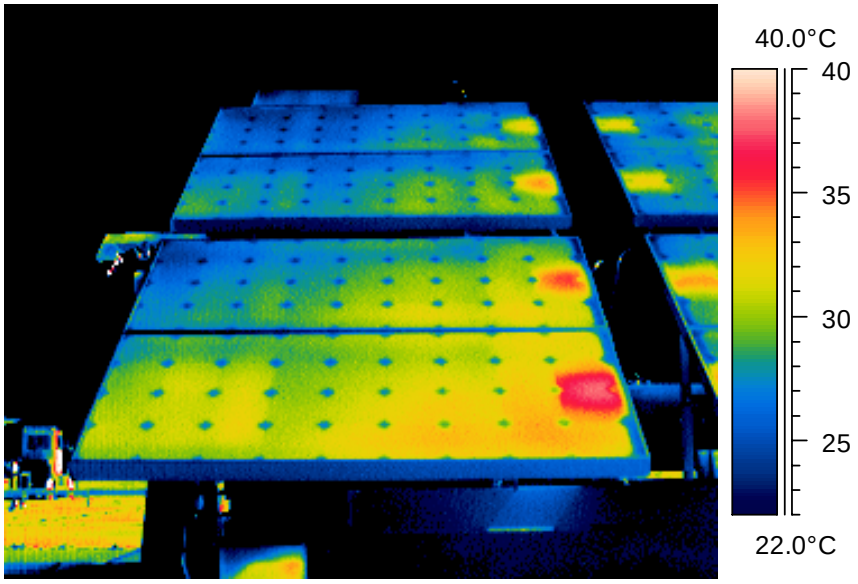

Figure 19. Thermal infrared (IR) image of several modules in an array illustrating the spatial variation in module temperature often present due to wind cooling, mounting structures, junction boxes, etc.

MODULE DATABASE

The module database available on Sandia's website, http://www.sandia.gov/pv, is a combination of performance parameters provided by module manufacturers and experimental data measured at Sandia National Laboratories. The rationale for including performance information from both sources is discussed below. This combination of parameters (coefficients) coupled with the Sandia performance model will enable analysts to closely simulate module and array performance characteristics over a wide range of operating conditions. The module database also includes general information such as cell technology and size, module dimensions and weight, maximum array voltage and fuse size, and other features. Figure 20 illustrates a data set for a typical module entry.

Specification sheets from module manufacturers provide performance parameters at a Standard Reporting Condition (SRC) defined by the American Society for Testing and Materials (ASTM) [18]. The SRC provides a single well-defined reference condition for testing and reporting module performance. Using our model, performance for all other operating conditions can be derived based on performance at the standard reference condition. The Standard Reporting Condition is defined to have 1000 W/m^2 solar irradiance, a standard solar spectrum representing a clear mid-day condition (air mass = 1.5), cell temperature inside the module of 25°C, and solar irradiance perpendicular (normal) to the module front surface. Two AM=1.5 solar spectra have been standardized by ASTM, one for testing flat-plate modules [24] and the other for concentrator modules [25]. In addition, internationally recognized calibration standards (World Photovoltaic Scale, WPVS) have been established in an attempt to encourage worldwide consistency in module performance measurement [26].

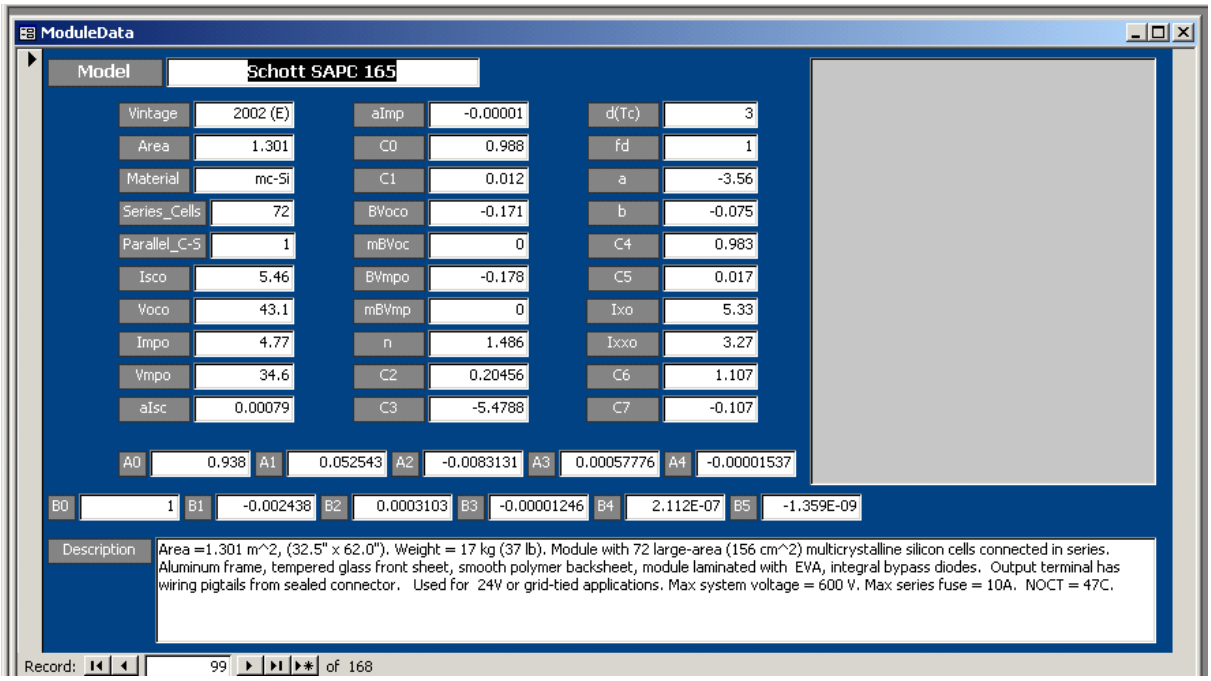

Figure 20. Example data entry in the module database associated with the array performance model.

Module manufacturers have fabricated and measured the performance of typically thousands of modules, and as a result they should have a good understanding of the statistical distribution of performance associated with their products. In addition, manufacturers all have the opportunity to use "reference" cells or modules calibrated through recognized testing organizations such as Sandia National Laboratories, the National Renewable Energy Laboratory (NREL), the Fraunhofer Institute in Germany, the European Solar Testing Institute (ESTI) in Italy, Advanced Industrial Science and Technology Institute (AIST) in Japan, and others. These reference cells should make it possible for manufacturers to measure and specify the performance of their modules with an uncertainty of less than ±5%. Therefore, the module database assumes that the manufacturer's stated performance parameters at Standard Reporting Conditions (SRC) are accurate.

In the database, the four basic performance parameters at the SRC are short-circuit current, open-circuit voltage, current at the maximum-power point, and voltage at the maximum-power point, and they are labeled I_{sco}, V_{oco}, I_{mpo}, and V_{mpo}, respectively. If an "(E)" is present in the 'Vintage' column of the database, then the 'expected' values for these four parameters were taken from the manufacturer's specification. If the "(E)" is not present, then the four basic performance parameters were measured at Sandia for modules of the same type, and in this case Sandia recognizes that the modules tested may or may not be representative of the manufacturers' production average. In all cases, the remaining parameters for each module in the database were based on Sandia test results; i.e. temperature coefficients, current and voltage versus irradiance coefficients, solar spectral coefficients, and angle-of-incidence coefficients.

Many of the parameters in the module database, such as the air mass coefficients and temperature coefficients for I_{sc} and I_{mp} can often be considered generic to all modules from a given module manufacturer, as long as the modules use the same cell type. The angle-of-incidence (AOI) coefficients can also be considered generic for all flat-plate modules with a glass front surface. However, the AOI coefficients will differ significantly for concentrator modules and for flat-plate modules with a non-glass front surface. For concentrator modules, the AOI coefficients are used to quantify the effect of solar tracking error on performance.

Manufacturers' specification sheets also provide vintage, total area, cell material type, and the wiring configuration of individual cells in the module. Many cells are typically connected in series, comprising a "cell-string." Multiple cell-strings may then be connected in parallel electrically to obtain higher current levels from the module. The module database indicates the number of cells in a cell-string, N_s, and the number of parallel cell-strings, N_p.

The Sandia performance model includes an empirically based expression that relates cell temperature to solar irradiance, ambient temperature, and wind speed. Two empirically determined coefficients and an estimate of the temperature difference between the cell and the module back surface are used in this thermal model. The coefficients given in the database are appropriate for the most common mounting configuration, namely modules mounted on an open rack with both surfaces exposed to ambient air. The thermal model is appropriate for other mounting configurations, for example directly attached to a roof surface, but different coefficients appropriate to the situation must be determined.

HISTORY OF SANDIA PERFORMANCE MODEL

As photovoltaic module technologies were evolving in the mid 1980s, Sandia developed a performance model, called PVFORM, for evaluating the expected energy production and economics associated with generic photovoltaic system designs in different geographic locations [27]. This model used the TMY solar resource and weather databases, had a thermal model for predicting module operating temperature, and had provisions for both fixed and solar tracking arrays. However, at that time the electrical performance model used for the photovoltaic modules was relatively simplistic, not addressing solar spectral influence, optical effects related to solar angle-of-incidence, and irradiance dependent electrical characteristics that are module design and module technology specific.

Starting in 1991, a concerted module testing effort was established at Sandia aimed at understanding and quantifying the interacting environmental influences that affect the performance of commercial photovoltaic modules. This effort led to the initial form of the Sandia performance model, which was first publicly presented at a Performance and Reliability Workshop at the National Renewable Energy Laboratory (NREL) in 1994, with an updated form presented at the NREL/SNL Program Review Meeting in 1996. From 1991 to 2003, the modeling approach was continuously validated using thousands of outdoor performance measurements on a wide variety of photovoltaic module technologies. Module technologies to which the methodology has been successfully applied include: crystalline silicon, multi-

crystalline silicon, poly-crystalline silicon-film, EFG multi-crystalline silicon, amorphous silicon, cadmium telluride, copper indium diselenide, silicon and GaAs concentrator modules, thin-film crystalline silicon on glass, crystalline-silicon “sliver” cells, and heterojunction crystalline silicon.

Beginning in September 1995, the same outdoor testing procedures and modeling methodology were applied in the field to a variety of large photovoltaic arrays. From 1995 to 1999, the performance model was successfully applied to more than a dozen photovoltaic arrays of different technologies, comprising over 1 MW of capacity. In 1997, a joint effort with Endecon Engineering was conducted that compared the Sandia testing and modeling procedures with those used at PVUSA in Davis, CA, for five large arrays with different module technologies [6].

In 1998, the performance model was incorporated in a prototype software program (PVMOD) at Sandia for conducting system analyses based on daily, monthly, and annual energy production. Also in 1998, the performance model and its associated test procedures were adopted by the National Institute of Standards and Technology (NIST) for use in their building integrated photovoltaic (BIPV) test laboratory [8]. In 1999, Sandia personnel started formatting and documenting the model and associated test procedures for possible inclusion in the developing IEEE 1479 standard "Recommended Practice for the Evaluation of Photovoltaic Module Energy Production." In 2000, Sandia and NREL conducted an extensive effort to validate their different module performance models by comparative analysis of year long data sets recorded at NREL for 5 different module technologies.

Beginning in 1998, a collaborative effort with Maui Solar Energy Software Corporation led to the inclusion of the Sandia performance model in a photovoltaic system design program developed by Maui Solar (PV-DesignPro) [11]. A second program, IVTracer, used to demonstrate the Sandia model and to translate field I-V measurements to Standard Reporting Conditions also resulted from the collaboration. In 2003, Maui Solar developed hardware and software that continuously monitor system performance by comparing measured performance to expected performance predicted by the model [28].

CONCLUSION

The performance model described in this document has evolved over many years at Sandia National Laboratories, and it has been extensively applied and validated for virtually all photovoltaic technologies now commercially available. It is our hope that this document provides enough detail for others to understand and to implement the array performance model in a manner most applicable to their needs.

REFERENCES

[1] D. King, W. Boyson, and J. Kratochvil, "Analysis of Factors Influencing the Annual Energy Production of Photovoltaic Systems," *29th IEEE PV Specialists Conference*, 2002.

[2] D. King, J. Kratochvil, and W. Boyson, "Measuring Solar Spectral and Angle-of-Incidence Effects on PV Modules and Solar Irradiance Sensors," *26th IEEE PV Specialists Conference*, 1997, pp. 1113-1116.

[3] D. King, J. Kratochvil, and W. Boyson, "Temperature Coefficients for PV Modules and Arrays: Measurement Methods, Difficulties, and Results," *26th IEEE PV Specialists Conference*, 1997, pp. 1183-1186.

[4] D. King and P. Eckert, "Characterizing (Rating) Performance of Large PV Arrays for All Operating Conditions," *25th IEEE PV Specialists Conference*, 1996, pp. 1385-1388.

[5] D. King, J. Kratochvil, and W. Boyson, "Field Experience with a New Performance Characterization Procedure for Photovoltaic Arrays," *2nd World Conference on PV Solar Energy Conversion*, Vienna, 1998, pp. 1947-1952.

[6] C. Whitaker, T. Townsend, J. Newmiller, D. King, W. Boyson, J. Kratochvil, D. Collier, and D. Osborn, "Application and Validation of a New PV Performance Characterization Method," *26th IEEE PV Specialists Conference*, 1997, pp. 1253-1256.

[7] B. Kroposki, W. Marion, D. King, W. Boyson, and J. Kratochvil, "Comparison of Module Performance Characterization Methods," *28th IEEE PV Specialists Conference*, 2000, pp. 1407-1411.

[8] A. H. Fanney, et al., "Short-Term Characterization of Building Integrated Photovoltaic Modules", Proceedings of Solar Forum 2002, Reno, NV, June 15-19, 2002.

[9] D. King, T. Hund, W. Boyson, and J. Kratochvil, "Experimental Optimization of the Performance and Reliability of Stand-Alone Photovoltaic Systems," *29th IEEE PV Specialists Conference*, 2002.

[10] D. King, et al., "Experimental Optimization of the FireFly 600 Photovoltaic Off-Grid System," Sandia National Laboratories Report, SAND2003-3493, October 2003.

[11] Maui Solar Energy Software Corporation, *Solar Design Studio Ver. 5.0: PV-DesignPro and IVTracer*, http://www.mauisolarsoftware.com

[12] R. Sullivan and F. Winkelmann, "Validation Studies of the DOE-2 Building Energy Simulation Program – Final Report," Lawrence Berkeley National Laboratory, LBL-42241, June 1998.

[13] D. Balcomb and G. Beeler, "Designing Low-Energy Buildings with Energy-10," Proc. Solar '98, 24th Passive Solar Conference, American Solar Energy Society, Albuquerque, 1998.

[14] Anon., "NSRDB Vol.2, National Solar Radiation Data Base, 1961-1990, NREL/TP-463-5784, 1995. Data available at National Renewable Energy Laboratory website: http://www.nrel/gov

[15] METEONORM, Global Meteorological Database for Solar Energy and Applied Climatology, Ver. 50, Edition 2003 http://www.meteotest.ch/en/firma

[16] R. Perez, et al., "Modeling daylight availability and irradiance components from direct and global irradiance," Solar Energy, Vol. 44, No. 5, (1990), pp. 271-289.

[17] J. Duffie and W. Beckman, Solar Engineering of Thermal Processes, Second Edition, John Wiley & Sons, 1991.

[18] ASTM E 1036, "Testing Electrical Performance of Non-concentrator Photovoltaic Modules and Arrays Using Reference Cells," American Society for Testing and Materials.
[19] R. Downs, et al., "PVUSA Procurement, Acceptance, and Rating Practices for Photovoltaic Power Plants," Pacific Gas and Electric Company R&D Report #95-30910000.1, Sept. 1995.
[20] M. K. Fuentes, "A Simplified Thermal Model of Photovoltaic Modules," Sandia National Laboratories Report, SAND85-0330, 1985.
[21] B. Marion, S. Rummel, and A. Anderberg, "Current-Voltage Translation using Bilinear Interpolation," submitted for publication in Progress in Photovoltaics journal, Nov. 2003.
[22] D. King and D. Myers, "Silicon-Photodiode Pyranometers: Operational Characteristics, Historical Experiences, and New Calibration Procedures," *26th IEEE PV Specialists Conference*, 1997.
[23] D. King, W. Boyson, and B. Hansen, "Improved Accuracy for Low-Cost Solar Irradiance Sensors," *2nd World Conference on PV Solar Energy Conversion*, Vienna, 1998, pp. 2001-2004.
[24] ASTM E 892, "Terrestrial Solar Spectral Irradiance at Air Mass 1.5 for a 37º Tilted Surface," American Society for Testing and Materials.
[25] ASTM E 891 "Terrestrial Direct Normal Solar Spectral Irradiance for Air Mass 1.5," American Society for Testing and Materials.
[26] C. R. Osterwald, et al., "The World Photovoltaic Scale: An International Reference Cell Calibration Program," *Prog. Photovolt: Res. Appl*. **7**, 1999, pp. 287-297.
[27] D. F. Menicucci, "Photovoltaic Array Performance Simulation Models," *Solar Cells*, **18** (1986).
[28] Personal communication with Michael Pelosi, Maui Solar Energy Software Corporation, regarding "GridTools" hardware/software for monitoring system performance. http://www.mauisolarsoftware.com

DISTRIBUTION LIST

MS-0703 PV Department Files (50 copies)
MS-0703 PV Department Library (5 copies)
MS-9018 Central Technical Files, 8945-1 (1 copy)
MS-0899 Technical Library, 9616 (2 copies)